Effect of Re-Deposition Layers in Plasma-Facing Wall on Tritium Retention and Tritium Depth Profile

Masao MATSUYAMA, Hideki ZUSHI[1)], Kazutoshi TOKUNAGA[1)], Arseniy KUZMIN[2)] and Kazuaki HANADA[1)]

Hydrogen Isotope Research Center, Organization for Promotion of Research, University of Toyama, 3190 Gofuku, Toyama 930-8555, Japan

[1)]*Rearch Institute for Applied Mechanics, Kyushu University, 6-1 Kasuga-Koen, Kasuga, Fukuoka 816-8580, Japan*

[2)]*National Institute for Fusion Science, Toki, Gifu 509-5292, Japan*

(Received 25 October 2018 / Accepted 4 June 2019)

Effect of the re-deposition layers formed on plasma-exposed stainless steel type 316L (SS316L) in QUEST on the retention and depth profile of tritium has been studied by both methods of tritium exposure experiments and numerical analyses of X-ray spectra observed by the β-ray-induced X-ray spectrometry (BIXS). Both samples of plasma-exposed and non-exposed SS316L were exposed to tritium gas under given temperature, time and pressure conditions. Surface of the former sample was covered with re-deposition layers after exposing to the plasma experiments. After tritium exposure, X-ray spectra induced by β-rays emitted from tritium atoms retained in the surface layers and/or dissolved into the bulk were measured using an ultra-low energy X-ray detector consisting of pure Ge semiconductor, and numerical analysis of the observed spectrum was conducted to estimate a tritium depth profile in the sample. As a result, it was found that the amount of tritium in surface layers of the plasma-exposed sample was about five times larger than that of the non-exposed sample, and the tritium depth profile for the plasma-exposed sample was about half depth in comparison with that for the non-exposed sample although the degassing temperature and tritium exposure conditions were the same for both samples. It was suggested, therefore, that the re-deposition layers played a role of diffusion barrier of tritium atoms formed on the sample surface.

Keywords: tritium retention, tritium depth profile, re-deposition layers, β-ray-induced X-ray spectrum, numerical analysis

DOI: 10.1585/pfr.14.1405125

1. Introduction

Reduction of fuel particles in the plasma-facing materials (PFMs) of the future fusion plants is one of the crucial issues from viewpoint of steady-state operation. In particular, tritium retention in PFMs is one of important issues from viewpoints of safety and economy as well as a site limitation of tritium. It is well known that original surface characteristics of PFMs change by bombardment of high energy particles such as neutron and fuel particles, by surface erosion due to physical and chemical sputtering, and by formation of re-deposition layers during a long operation [1]. Therefore, tritium retention in the PFMs should be strongly affected by various phenomena. Especially, the re-deposition layers formed on the surface of PFMs directly influence to adsorption/desorption behavior of tritium as was reported by previous papers [2, 3]. Namely, physical and chemical properties of original surfaces of PFMs are changed by the re-deposition layers, and new surface characteristics will appear. It is foreseen, therefore, that tritium retention in surface layers changes depending on a state of plasma and vacuum conditions of the fusion devices. The diffusion behavior of tritium in the PFMs will be similarly affected by the formation of re-deposition layers.

Matsuyama *et al.* reported the effects of plasma exposure on tritium retention in a stainless steel type 316L (SS316L) [4, 5]. The samples used in this study were exposed to plasmas of the Large Helical Device (LHD) in National Institute for Fusion Research and of the Q-shu University Experiment with Steady-State Spherical Tokamak (QUEST) [5]. The device of QUEST was established in the Research Institute for Applied Mechanics (RIAM) of Kyushu University. Non-exposed SS316L (described hereafter as "bare SS316L") samples were also used in these studies to examine tritium retention behavior in detail. The amount of tritium retained in the plasma-exposed SS316L samples was rather large in comparison with that in the bare SS316L samples, when the samples were exposed to tritium gas at 393 K after degassing at the same temperature. This may be due to the effect of re-deposition layers formed by plasma exposure.

On the other hand, the tritium retention in surface layers of specimens increased with increasing both tempera-

author's e-mail: toyama3h1949@gmail.com

tures of degassing and tritium exposure [5]. When a degassing temperature was above 573 K, significant increase in tritium retention appeared even if tritium exposure temperature was low. Similar tendency of tritium retention was observed for the bare SS316L samples. Namely, this indicates that the surface state of SS316L plays an important role for tritium retention. Analyses by X-ray photoelectron spectroscopy (XPS) indicated that changes in the chemical states of SS316L surface at high temperatures were strongly related to tritium retention behavior. It was concluded, therefore, that the tritium retention in PFMs was significantly affected by history of the evacuation conditions along with re-deposition layers formed by exposing to plasmas. In addition to such a heating effect, distribution of tritium near surface of a specimen is of an important issue to discuss about recycling of fuel particles in PFMs.

Many studies on a depth profile of tritium in metallic materials such as stainless steels have been reported so far [6–10]. Most of these papers showed that tritium atoms absorbed in the materials are trapped in surface layers of a few micrometers in thickness and that tritium concentration in this region could be more than two orders of magnitude higher than that in the bulk [7–10]. Therefore, determination of a tritium depth profile in the materials is of an important factor to consider recycling of tritium in the surface layers of PFMs even if the total amount of tritium retained in PFMs is the same. There are no reports about the effects of re-deposition layers formed by plasma exposure on the retention and depth profile of tritium.

Some techniques are employed for determination of a depth profile of hydrogen isotope atoms such as H and D atoms trapped in the metallic materials. For example, nuclear reaction analysis such as $H(^{15}N, \alpha\gamma)^{12}C$ and $D(^{3}He, p)^{4}He$ is applicable to date as a non-destructive technique for measurement of a depth profile of hydrogen isotopes in surface layers of the materials [11–14]. On the other hand, an etching method of surface layers by acid solution is principally available for the tritium containing samples although this technique is destructive and generates the radioactive liquid waste [7, 8]. As a quite different method from these techniques, Matsuyama has proposed a new method for estimation of a tritium depth profile in the tritium retained specimens [15]. Although the details will be described later, the new method is a technique using an X-ray spectrum induced by β-rays which are emitted by the decay of tritium atoms on the surface and in the bulk of metallic materials. This technique is non-destructive method for analysis of a tritium depth profile, and is called as BIXS (β-ray induced X-ray spectrometry).

From these viewpoints, effect of the re-deposition layers on the retention and depth profile of tritium has been examined in this study from both sides of measurements of X-ray spectra and their reproduction by applying numerical analyses based on a given depth profile of tritium. The re-deposition layers were formed on the surface of SS316L specimen by exposing to plasmas in QUEST.

2. Experimental

2.1 Materials

The sample plates used are stainless steel type 316L, whose nominal atomic composition (at. %) was as follows: Fe(65.3), Cr(19.0), Ni(11.9), Mn(1.89), Mo(1.28) and Si(0.72). Size of a plate was $15 \times 15 \times 0.5\,mm^3$. It was polished by a buff and then rinsed with acetone. Two kinds of SS316L samples were used in this study: one is a bare SS316L sample and the other is a plasma-exposed SS316L sample. It was prepared by the following procedures: a bare SS316L sample was fixed by a sample holder attached at the top of the linear motion feed through, and it was inserted near inner wall of QUEST. A linear motion feed through was connected with the MH10 port which is located at mid-plane of QUEST. The sample was mainly exposed to hydrogen plasmas during a plasma experiment campaign (ID No. 450-460) of the spring/summer season in 2016. After the plasma exposure to a bare SS316L sample, it was transported from the facility of QUEST in Kyushu University to the tritium experiment facility of Hydrogen Isotope Research Center, University of Toyama. Tritium gas diluted with hydrogen was used for tritium exposure experiments, and the concentration of tritium used was ca. 5% tritium. Powdered Zr-Ni alloy which is well known as a hydrogen storage material was used for the supply/recovery process of tritium gas.

2.2 Procedures

Tritium exposure tests of the plasma-exposed and bare SS316L samples were conducted under given conditions of temperature and pressure by using a specially designed tritium exposure device [16]. A given pressure of tritium gas was supplied to a tritium exposure part by heating Zr-Ni alloy powders at a given temperature and it was completely recovered by using the same Zr-Ni alloy powders after exposure to tritium gas. Temperature and pressure in the tritium exposure tests were set at 623 K and 1.3 kPa, respectively. Tritium gas was exposed a sample for 4 hr in each run. After the exposure, the sample was quickly cooled down at room temperature, and the residual tritium gas in the exposure part was recovered. Subsequently, evacuation of the exposure part by an ion pump was continued for one night to avoid the tritium contamination of ambient air when the exposure part was opened to take out the tritium exposure sample.

After the tritium exposure and evacuation, the sample was taken out and the amount of tritium retained in a sample was evaluated by using the technique of BIXS, where argon was used as a working gas. The X-ray spectra were measured by an ultra-low energy X-ray detector. In order to detect low energy X-rays higher than 1 keV, a thin beryllium plate (*ca.* 8 μm in thickness) was employed as an entrance window material of the X-ray detector. Electrical signal of the X-rays was accumulated for a given time by a multi-channel analyzer, and energy width (ΔE) in each

channel was set to $\Delta E = 32.8$ eV.

The amount of tritium retained in surface layers can be evaluated from the intensity of characteristic X-rays of Ar($K_{\alpha,\beta}$), which means the sum of X-ray intensities of Ar(K_α) and Ar(K_β). Thickness of the surface layers was defined as an average escape depth of β-rays in SS316L. It was estimated to be 0.22 μm for 5.7 keV which is the average energy of β-rays and 0.07 μm for 3.2 keV which is the energy of K-shell absorption edge of Ar. On the other hand, depth profile of tritium in the bulk was estimated by applying numerical analysis of the X-ray spectrum observed. Shape of bremsstrahlung X-ray spectrum in the observed X-ray spectrum gives important information about the depth profile of tritium. How to analyze an X-ray spectrum is described in detail elsewhere [15].

3. Numerical Analysis of Tritium Depth Profiles Based on BIXS

β-rays emitted from nuclei of tritium atoms have continuous energies in the range from 0 to 18.6 keV. When tritium atoms exist in the bulk of a material, most of kinetic energy of β-rays is consumed by the interactions with constituent atoms of a material. Consumed energies are partly converted into characteristic and bremsstrahlung X-rays in a material. The former X-rays show a line spectrum, while the latter ones do the continuous spectrum. Although penetration power of the X-rays induced by β-rays is much greater than that of the β-rays, the produced X-rays are partly absorbed in a material because these are low energy X-rays. Therefore, practical intensity of an X-ray spectrum observed at the surface of a material depends on not only the number of tritium atoms but also a depth profile of tritium atoms in the material. This is a reason why shape of a bremsstrahlung spectrum changes with a depth profile of tritium in materials.

As an example, X-ray spectra obtained by a numerical calculation method are shown in Fig. 1, assuming that a given amount of tritium dissolves into a SS316L sample. Depth profiles of tritium as shown in Fig. 2 were given in each calculation. In addition, it was assumed that a penetration depth of β-rays in SS316L was 0.22 μm as mentioned above. Appearance of the plural characteristic X-ray peaks and a broad and weak peak was confirmed in the spectra of Fig. 1. The latter peak is bremsstrahlung X-rays and the maximum shifts to higher energy side with extension of a tritium depth profile. Namely, it can be understood that the shape of bremsstrahlung X-ray spectrum depends on a depth profile of tritium in a SS316L sample.

Appearance of two peaks around 3 keV is due to a reason that argon gas (Ar(K_α) = 2.957 and Ar(K_β) = 3.190 keV) was used as a working gas of BIXS in the calculation of an X-ray spectrum. The peak of Ar(K_α) consists of Ar($K_{\alpha1}$) (= 2.9577 keV) and Ar($K_{\alpha2}$) (= 2.9556 keV) peaks. As the energy difference between these peaks is very small as 2.07 eV, it is impossible to separate both X-ray peaks by the present X-ray detector. As a working gas, other gases such as neon, krypton, and xenon are also applicable to measure tritium retained in the sur-

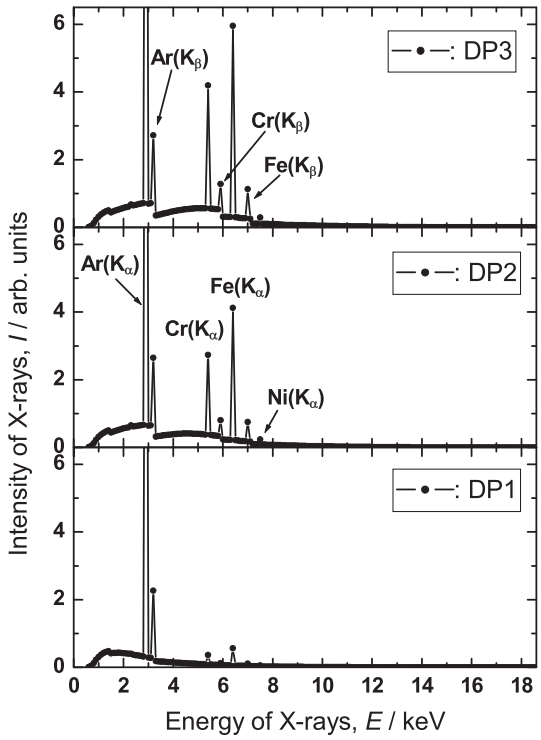

Fig. 1 X-ray spectra calculated by basing on the different depth profiles of tritium in bare SS316L. Tritium depth profiles from DP1 to DP3 are shown in Fig. 2.

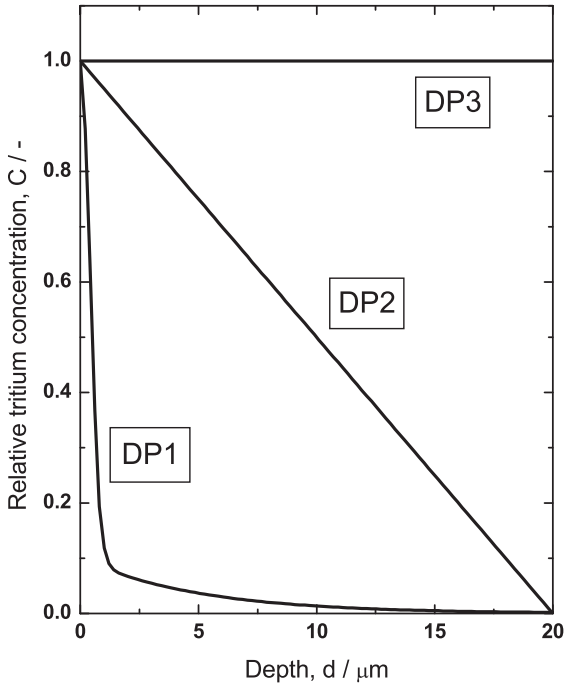

Fig. 2 Example of various depth profiles of tritium assumed for numerical calculation of X-ray spectra. DP1: exponential function, DP2: first order function, DP3: uniform distribution.

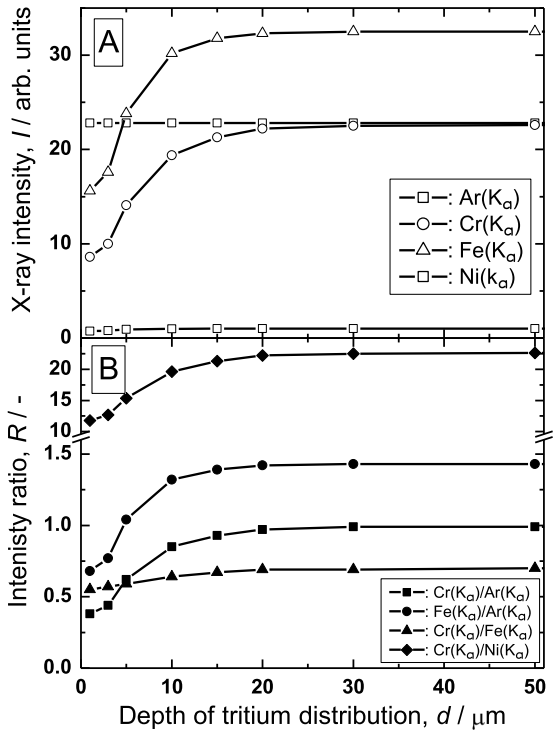

Fig. 3 Change in the intensities of characteristic X-rays and intensity ratios among them with depth of tritium distribution. Figure [A] shows changes in X-ray intensity and Fig. [B] shows changes in intensity ratio with the depth of uniform tritium distribution.

face layers, but argon gas is the best among them from viewpoints of economy and safety. This is a reason why argon gas was used in this study. By using a working gas, it is possible to separate tritium retained in the surface layers from tritium dissolved into the region deeper than 0.2 μm. One can apply other working gases such as helium, nitrogen and oxygen when major purpose is to measure only a bremsstrahlung X-ray spectrum.

The intensities of plural characteristic X-ray peaks obtained from numerical calculation for a SS316L sample and ratios among them give important information to estimate qualitatively a tritium depth profile. Figure 3[A] shows changes in the intensities of Ar(K_α), Cr(K_α), Fe(K_α) and Ni(K_α) for the uniform depth profile of DP3 in Fig. 2. And the ratios Cr(K_α)/Ar(K_α), Fe(K_α)/Ar(K_α), Cr(K_α)/Fe(K_α), and Cr(K_α)/Ni(K_α) were also described in Fig. 3[B]. It is seen from Fig. 3[A] that intensities of characteristic X-rays steeply increase with an increase in depth but those saturate at about 30 μm. This is also applicable to the ratios among them although increase in the ratio Cr(K_α)/Fe(K_α) is somewhat moderate in comparison with other ratios. Such a different increase behavior may be mainly due to the large mass absorption coefficient of Fe(K_α) X-rays for chromium atoms.

4. Results and Discussion

Figure 4 shows an example of X-ray spectrum observed for a bare SS316L sample. This sample was exposed to tritium gas at 623 K for 4 hr after degassing at 673 K in vacuum. As clearly seen from the spectrum, plural characteristic X-ray peaks such as Ar($K_{\alpha,\beta}$), Cr(K_α) and Fe(K_α) and a broad bremsstrahlung X-ray peak of which maximum was around 5.5 keV were observed, indicating that much tritium adsorbed on the sample surface and a part of the adsorbed tritium diffused into bulk during exposure to tritium gas.

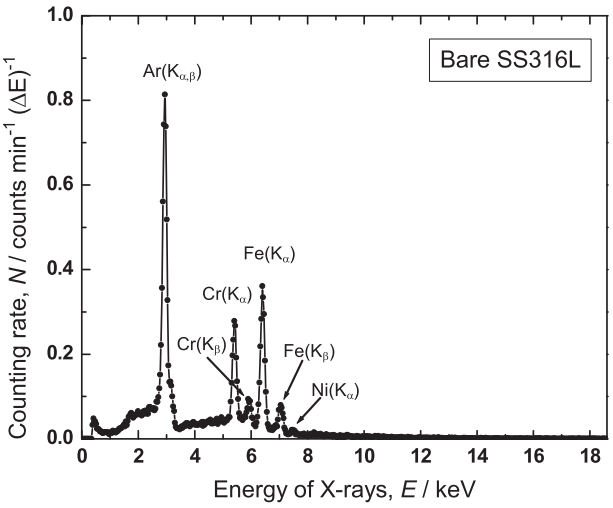

Fig. 4 X-ray spectrum observed for the bare SS316L sample exposed to tritium gas. Tritium exposure conditions: degassing temperature was 673 K and tritium exposure temperature was 623 K.

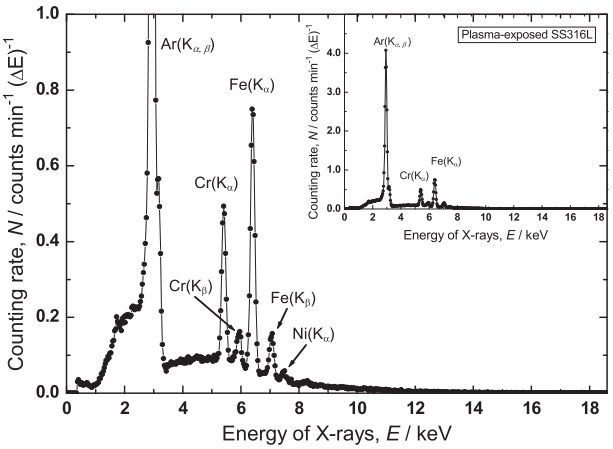

Fig. 5 X-ray spectrum observed for the plasma-exposed SS316L sample. Tritium exposure conditions: degassing temperature was 673 K and tritium exposure temperature was 623 K. The inset shows the whole X-ray spectrum observed in this experiment to compare with the X-ray spectrum showed in Fig. 4.

On the other hand, Fig. 5 shows the X-ray spectrum observed for a plasma-exposed sample. A similar X-ray spectrum was observed, although a peak intensity of

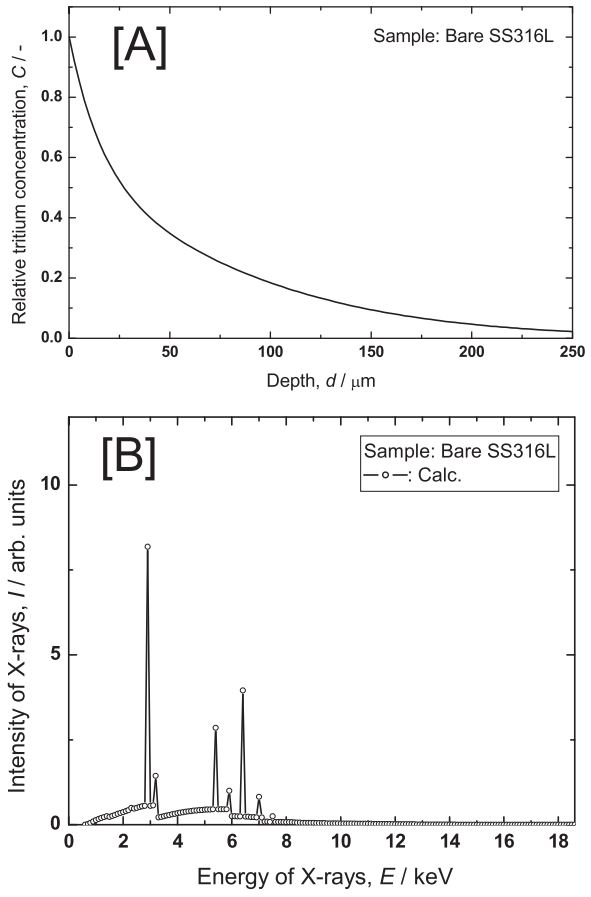

Fig. 6 Analysis of tritium depth profile for the bare SS316L exposed to tritium gas: [A] is an assumed depth profile, [B] is the X-ray spectrum calculated by basing on the depth profile shown in [A].

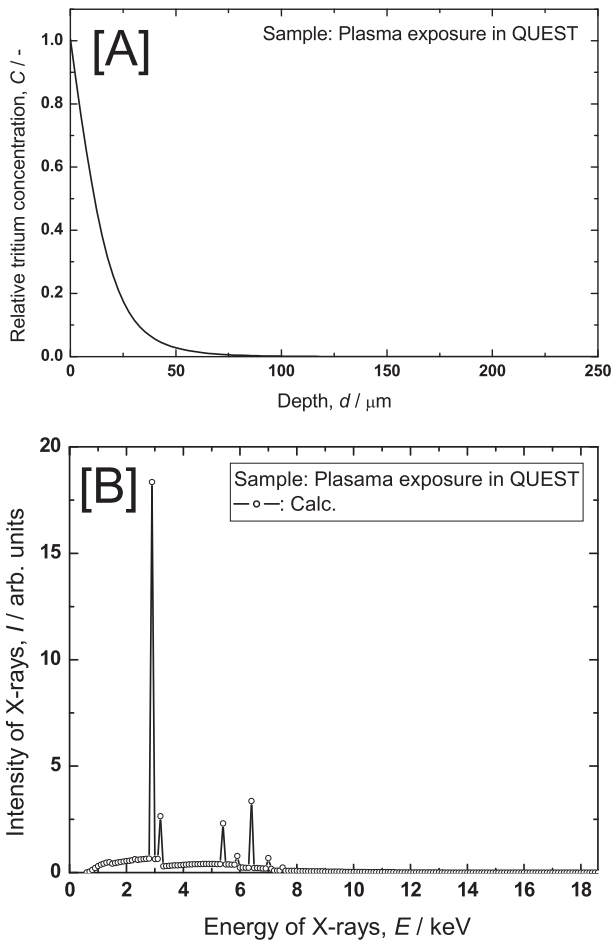

Fig. 7 Analysis of tritium depth profile for the plasma-exposed sample: [A] is an assumed depth profile, [B] is the X-ray spectrum calculated by basing on the depth profile shown in [A].

the X-rays was different from that observed in Fig. 4 as shown in the inset of Fig. 5. Especially, intensity of the Ar($K_{\alpha,\beta}$) peak which is proportional to the amount of tritium retained in surface layers increased by a factor of *ca.* 5, whereas the intensities of bremsstrahlung, Cr(K_α) and Fe(K_α) X-rays did not increase significantly. Such tendency indicates that the amount of tritium retained in the surface layers largely increased but the bulk concentration was not so high. This indicates that diffusion of tritium into the re-deposition layers formed on the surface is low. It is well known that the plasma-exposed sample is covered with re-deposition layers such as carbon and the oxides of constituent elements of plasma-facing materials [1]. Namely, the re-deposition layers bring about increase in the amount of tritium in surface layers and at the same time those prevent diffusion of tritium into the bulk. It is considered, therefore, that the former effect may give rise to apparent increase in the recycling ratio of fuel particles on the surface of PFMs.

It is possible to estimate a depth profile of tritium in the materials by analyzing the observed X-ray spectra as mentioned in the previous section. Namely, one can approximately reproduce the observed X-ray spectrum when a reasonable depth profile is given. Thus X-ray spectra were repeatedly calculated by assuming various depth profiles of tritium. Figure 6[A] shows one of tritium depth profiles assumed for the bare SS316L sample, and Fig. 6[B] describes the X-ray spectrum which was calculated basing on the depth profile described in Fig. 6[A]. Table 1 shows the summary of peak intensities of the characteristic X-rays in the observed and simulated spectra. As clearly seen from the intensity ratio of both spectra, the ratios were almost 0.5. In addition, intensity ratios of a major peak in the simulation spectrum were in accord with that in the observed spectrum within 10%. Namely, these values mean that the characteristic X-ray peaks observed for bare SS316L sample were perfectly reproduced by numerical calculation. On the other hand, the shape of a simulated bremsstrahlung X-ray peak also agreed with that of the observed peak except for a low energy region. It is seen, therefore, that the tritium depth profile of Fig. 6[A] was able to reproduce thoroughly the observed X-ray spectrum shown in Fig. 4. That is, it was found from the depth

Table 1 Summary of the peak intensity and ratio in the observed and simulated spectra for bare SS316L sample.

Specrum & Ratio	Peak intensity / cpm						Ratio of peak intensity		
	$Ar(K_{\alpha,\beta})$	$Cr(K_{\alpha})$	$Cr(K_{\beta})$	$Fe(K_{\alpha})$	$Fe(K_{\beta})$	$Ni(K_{\alpha})$	$Cr(K_{\alpha})/Ar(K_{\alpha,\beta})$	$Fe(K_{\alpha})/Ar(K_{\alpha,\beta})$	$Fe(K_{\alpha})/Cr(K_{\alpha})$
Observation	4.74	1.28	0.30	1.86	0.40	0.05	0.27	0.39	1.45
Simulation	8.67	2.40	0.64	3.71	0.6	0.17	0.28	0.43	1.55
Obs. / Simu.	0.5	0.5	0.5	0.5	0.7	0.3	1.0	0.9	0.9

*) cpm: counts per minute.

Table 2 Summary of the peak intensity and ratio in the observed and simulated spectra for plasma-exposed SS316L sample.

Spectrum & Ratio	Peak intensity / cpm						Ratio of peak intensity		
	$Ar(K_{\alpha,\beta})$	$Cr(K_{\alpha})$	$Cr(K_{\beta})$	$Fe(K_{\alpha})$	$Fe(K_{\beta})$	$Ni(K_{\alpha})$	$Cr(K_{\alpha})/Ar(K_{\alpha,\beta})$	$Fe(K_{\alpha})/Ar(K_{\alpha,\beta})$	$Fe(K_{\alpha})/Cr(K_{\alpha})$
Observation	23.3	2.15	0.51	3.9	0.61	0.14	0.09	0.17	1.81
Simulation	19.8	1.92	0.47	3.14	0.49	0.15	0.10	0.16	1.64
Obs. / Simu.	1.2	1.1	1.1	1.2	1.2	0.9	0.9	1.0	1.1

*) cpm: counts per minute.

profile that tritium atoms diffused near the center region in depth of a bare SS316L sample under the given temperature conditions.

Similar numerical calculations were applied to estimate a tritium depth profile for the plasma-exposed sample. The X-ray spectrum was repeatedly calculated in the same manner by assuming various depth profiles of tritium. Figure 7[A] shows one of tritium depth profiles assumed for numerical calculation. Figure 7[B] is the X-ray spectrum calculated by assuming the depth profile shown in Fig. 7[A]. Figure 7[B] which is well coincident with the observed spectrum was obtained by applying the depth profile of Fig. 7[A]. Table 2 shows the summary of intensities of the characteristic X-ray peaks in the observed and simulated spectra. As clearly seen from the intensity ratio of both spectra, the ratio was almost constant as 1.1. In addition, intensity ratio of a major peak in the simulation spectrum was in accord with that in the observed spectrum within 10%. Namely, this means that the characteristic X-ray peaks observed for plasma-exposed sample were reproduced by numerical calculation. On the other hand, the shape of a simulated bremsstrahlung X-ray peak also agreed with that of the observed peak except for a low energy region. As clearly seen from the depth profile of Fig. 7[A], a region of tritium distribution became narrow although the exposure temperature conditions of tritium were the same as the bare SS316L sample, indicating that diffusion of tritium into bulk of the plasma-exposed sample was rather disturbed. It is likely that the decline of the diffusivity of tritium is due to the re-deposition layers formed on the surface of SS316L by exposure to plasmas. Namely, re-deposition layers play a role as a diffusion barrier of tritium although they bring about the increase in tritium retention in the surface layers.

5. Conclusions

Effect of plasma exposure on the retention and depth profile of tritium in stainless steel type 316L (SS316L) exposed to tritium gas has been examined by both methods of experiment and numerical calculation. The amount of tritium retained in surface layers of the plasma-exposed sample was about five times larger than that of the bare SS316L sample even if both samples were exposed to tritium gas under the same conditions. However, it was found from numerical calculation of X-ray spectrum induced by β-rays of the dissolved tritium that the tritium depth profile estimated from the plasma-exposed SS316L sample was narrower than that from the bare SS316L sample. It is likely that this is due to decline of diffusion rate of tritium atoms in the re-deposition layers formed on the sample surface by plasma exposure. Namely, it was concluded that re-deposition layers played a role as a diffusion barrier but those brought about the increase in potential of tritium retention in surface layers.

Acknowledgments

A part of this work has been performed with the support and under the auspices of the National Institute for Fusion Science (NIFS) Collaboration Research Program (NIFS12KUTR081).

[1] Z. Wang, K. Hanada, N. Yoshida, T. Shimoji, M. Miyamoto, Y. Oya, H. Zushi, H. Idei, K. Nakamura, A. Fujisawa, Y. Nagashima, M. Hasegawa, S. Kawasaki, A. Higashijima, H. Nakashima, T. Nagata, A. Kawaguchi, T. Fujiwara, K. Araki, O. Mitarai, A. Fukuyama, Y. Takase and K. Matsumoto, Rev. Sci. Instrum. **88**, 093502 (2017).
[2] M. Matsuyama, S. Abe, K. Nishimura, Y. Ono, Y. Oya, K. Okuno, T. Hino and A. Sagara, J. Plasma Fusion Res. SERIES **10**, 64 (2013).
[3] M. Matsuyama, S. Abe, Y. Ono, K. Nishimura, N. Ashikawa, Y. Oya, K. Okuno, T. Hino and A. Sagara, Plasma Fusion Res. **8**, 2405014 (2013).
[4] M. Matsuyama, S. Abe, K. Nishimura, N. Ashikawa, Y. Oya, K. Okuno, Y. Yamauchi, Y. Nobuta and A. Sagara, Plasma Fusion Res. **9**, 3405135 (2014).
[5] M. Matsuyama, H. Zushi, K. Tokunaga, A. Kuzmin and K. Hanada, Nucl. Mater. Energy **16**, 52 (2018).
[6] M. Matsuyama, Y. Torikai, M. Hara and K. Watanabe, Nucl. Fusion **47**, S464 (2007).
[7] Y. Torikai, R.-D. Penzhorn, M. Matsuyama and K. Watanabe, Fusion Sci. Technol. **48**, 177 (2005).
[8] Y. Torikai, R.-D. Penzhorn, M. Matsuyama and K. Watanabe, J. Nucl. Mater. **329-333**, 1624 (2004).
[9] A.N. Perevezentsev, K. Watanabe, M. Matsuyama and Y. Torikai, Fusion Sci. Technol. **41**, 746 (2002).
[10] R.D. Calder, T.S. Elleman and K. Verghese, J. Nucl. Mater. **46**, 46 (1973).
[11] A. Stern, D. Khatamian, T. Laursen, G.C. Weatherly and J.M. Perz, J. Nucl. Mater. **144**, 35 (1987).
[12] W. Möller and J. Bøttiger, J. Nucl. Mater. **88**, 95 (1980).
[13] W. Möller, P. Børgesen and J. Bøttiger, J. Nucl. Mater. **76-77**, 287 (1978).
[14] W.A. Lanford, H.P. Trautvetter, J.F. Ziegler and J. Keller, Appl. Phys. Lett. **28**, 566 (1976).
[15] M. Matsuyama, K. Watanabe and K. Hasegawa, Fusion Eng. Des. **39-40**, 929 (1998).
[16] M. Matsuyama and S. Abe, Fusion Eng. Des. **113**, 250 (2016).